

M agnetic F ield E ffect on the Superconducting M agnetic G ap of  $\text{Nd}_{1.85}\text{Ce}_{0.15}\text{CuO}_4$ E. M. Motoyama,<sup>1</sup> P. K. Mang,<sup>2</sup> D. Petitgrand,<sup>3</sup> G. Yu,<sup>1</sup> O. P. Vajk,<sup>4</sup> I. M. Vishik,<sup>1</sup> and M. G. Reven<sup>2,5,\*</sup><sup>1</sup>Department of Physics, Stanford University, Stanford, California 94305<sup>2</sup>Department of Applied Physics, Stanford University, Stanford, California 94305<sup>3</sup>Laboratoire Leon Brillouin (CEA-CNRS), CEA-Saclay, 91191 Gif-sur-Yvette Cedex, France<sup>4</sup>NIST Center for Neutron Research, National Institute of Standards and Technology, Gaithersburg, Maryland 20899<sup>5</sup>Stanford Synchrotron Radiation Laboratory, Stanford, California 94309

(Dated: February 8, 2022)

Inelastic neutron scattering measurements on the archetypical electron-doped material  $\text{Nd}_{1.85}\text{Ce}_{0.15}\text{CuO}_4$  up to high relative magnetic field strength,  $H/H_{c2} = 50\%$ , reveal a simple linear magnetic-field effect on the superconducting magnetic gap and the absence of field-induced in-gap states. The extrapolated gap-closing field value is consistent with the upper critical field  $H_{c2}$ , and the high-field response resembles that of the paramagnetic normal state.

PACS numbers: 74.25.Ha, 74.25.Nf, 74.72.Jt

A pivotal problem in condensed matter physics during the past two decades has been the determination of the ground state phase diagram of the high-temperature superconductors as a function of carrier density and magnetic field. Knowledge about the ground state that competes with the superconducting (SC) phase may be crucial to understanding the mechanism of superconductivity; this can be studied by suppressing superconductivity in a strong magnetic field, which leads to the formation of non-SC vortex regions embedded in the otherwise SC material [1].

The high- $T_c$  superconductors are divided into two classes, depending on whether they are formed by doping electrons or holes into the antiferromagnetic (AF) Mott insulator parent compounds [2]. In the hole-doped materials, the low-energy magnetic response is incommensurate and manifests itself in neutron scattering as four peaks situated symmetrically around the AF zone center ( $\pi, \pi$ ) [3]. Recent neutron-scattering studies in a magnetic field indicate that the non-SC ground state may be magnetically ordered [4, 5, 6, 7]. Specifically, in underdoped  $\text{La}_{2-x}\text{Sr}_x\text{CuO}_4$  (LSCO) and  $\text{La}_2\text{CuO}_{4+}$ , applying a magnetic field enhances the incommensurate spin density wave (SDW) order already present in the system [5, 6]. In optimally and slightly-overdoped LSCO, for which the magnetic signal is gapped (i.e., no static order) [8], a magnetic field induces new excitations below the gap energy [4, 7, 9]. The phase diagram thus contains a SC phase and a phase with coexisting SC and SDW order [10]. The overdoped system lies in the SC phase, and a magnetic field pushes it towards the SC + SDW phase. The underdoped system already lies in the SC + SDW phase at zero field. There exists a zero-field quantum critical point between these two phases. Interestingly, recent results at intermediate doping show that a relatively low magnetic field of  $H = 3\text{ T}$  pushes the system from the SC into the SC + SDW phase [11].

Upon doping, the electron-doped compounds exhibit a particularly robust neighboring AF phase in zero mag-

netic field [12], and the magnetic response remains commensurate at ( $\pi, \pi$ ) [13]. One might expect the phase diagram to be similar to the hole-doped case, with superconductivity coexisting with commensurate AF order instead of incommensurate SDW order. Initial experiments on  $\text{Nd}_{1.85}\text{Ce}_{0.15}\text{CuO}_4$  agreed with this naive picture: a magnetic field perpendicular to the  $\text{CuO}_2$  sheets was found to induce an elastic signal at ( $\pi, \pi$ ) [14]. However, it was subsequently shown that this signal is spurious: it is due to the paramagnetic response of the epitaxial secondary phase  $(\text{Nd;Ce})_2\text{O}_3$  [15, 16]. Consequently, the important question of the nature of the field-induced ground state on the electron-doped side of the phase diagram has remained open. We note that large crystals of SC NCCO typically contain a second spurious signal due to regions that have not been fully oxygen-reduced. These AF NCCO remnants have a three-dimensional or quasi-two-dimensional spatial extent, and they primarily contribute to the elastic response [16, 17]. While these chemical properties prevent a search for any genuine elastic signal, they do not prevent measurements of the inelastic response from the SC majority volume fraction. Indeed, a careful inelastic neutron scattering measurement on NCCO has clearly revealed the SC magnetic gap below  $T_c$  [13, 18].

In this Letter, we use inelastic neutron scattering to determine the magnetic field effect on this SC gap. For the hole-doped materials, the upper critical field at which superconductivity is completely destroyed is 50 T or greater [19], and hence prohibitively large for neutron scattering experiments. For the electron-doped materials, on the other hand,  $H_{c2}$  is relatively low ( $\sim 10\text{ T}$ ) [19], which has allowed us to observe a field effect on the SC magnetic gap in NCCO up to high values of relative magnetic field strength. We find that applying a magnetic field causes a rigid shift of the gap profile to lower energies. This contrasts the case of optimally-doped and overdoped LSCO, in which a magnetic field introduces in-gap states. A complementary zero-field measurement on

non-SC  $\text{Nd}_{1.85}\text{Ce}_{0.15}\text{Cu}_{0.985}\text{Ni}_{0.015}\text{O}_4$  demonstrates that the low-temperature spin correlations remain finite. Our findings imply a uniform low-energy magnetic response for fields below  $H_{c2}$ , and they are consistent with a paramagnetic ground state in the absence of superconductivity.

The inelastic neutron scattering experiment was carried out on the 4F2 triple-axis spectrometer at the Laboratoire Leon Brillouin in Saclay, France, with a nominal neutron energy of 14.7 meV and collimations of  $60^\circ$ -open-sample-open, and with a horizontally focusing monochromator and a vertically focusing analyzer. The  $\text{Nd}_{1.85}\text{Ce}_{0.15}\text{Cu}_{0.985}\text{Ni}_{0.015}\text{O}_4$  crystal (mass 5.0 g) was grown at Stanford University in an oxygen-flow at a pressure of 4 atm using the traveling-solvent coating-zone technique, and subsequently annealed for 10 hours at 970 °C in argon, followed by 500 °C for 20 hours in oxygen [16]. As shown in Fig. 1(a), the crystal exhibits an onset  $T_c$  of 22 K. A second, non-SC crystal of  $\text{Nd}_{1.85}\text{Ce}_{0.15}\text{Cu}_{0.985}\text{Ni}_{0.015}\text{O}_4$  (mass 3.1 g) was prepared by the same method and studied in zero field in two-axis mode [12]. These two-axis data were taken on the BT9 spectrometer at the NIST Center for Neutron Research, with an incident neutron energy of 14.7 meV and collimations  $40^\circ$ - $46^\circ$ -sample- $10^\circ$ . Inductively coupled plasma (ICP) analysis indicates that the composition of the Ni-doped crystal is close to its specified nominal values, while the Ce concentration of the Ni-free crystal is less uniform and closer to  $x = 0.16$ .

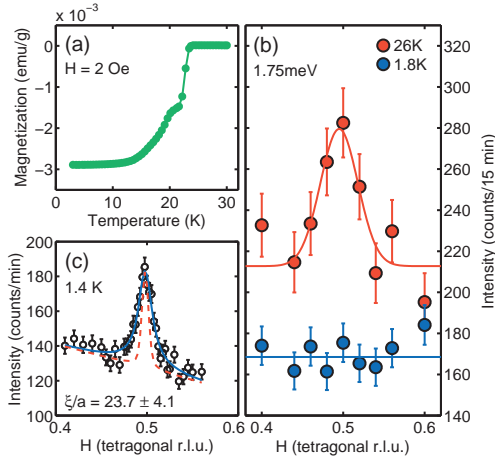


FIG. 1: (color online). (a) SQUID magnetometry of the whole  $\text{Nd}_{1.85}\text{Ce}_{0.15}\text{Cu}_{0.985}\text{Ni}_{0.015}\text{O}_4$  crystal used in the neutron scattering experiment showing an onset  $T_c$  of 22 K. (b)  $(H; 1 H; 0)$  scans through  $(l=2; l=2; 0)$  at an energy transfer of  $\hbar = 1.75$  meV in  $\text{Nd}_{1.85}\text{Ce}_{0.15}\text{Cu}_{0.985}\text{Ni}_{0.015}\text{O}_4$  above ( $T = 26$  K) and well below ( $T = 1.8$  K)  $T_c$ . (c) Determination of the instantaneous spin correlation length at  $T = 1.4$  K in non-SC  $\text{Nd}_{1.85}\text{Ce}_{0.15}\text{Cu}_{0.985}\text{Ni}_{0.015}\text{O}_4$  using the energy-integrating two-axis scan [12]. The data are fit (continuous line) to a Lorentzian convoluted with the calculated resolution function (dashed line).

NCCO has a tetragonal unit cell (space group  $I4/mmm$ ) with low-temperature lattice constants  $a = 3.94$  Å and  $c = 12.09$  Å for  $x = 0.15$ . We represent wavevectors as  $(H; K; L)$  in reciprocal lattice units (r.l.u.), where  $Q = (2H/a; 2K/a; 2L/c)$ . The AF zone center at  $(l=2; l=2; 0)$  is also represented as  $(; ; )$  (i.e.,  $a$   $1$ ). The inelastic experiments on SC NCCO were performed in the  $(H; K; 0)$  geometry, in which the crystal  $c$ -axis is perpendicular to the scattering plane. The magnetic field was applied vertically in the  $c$  direction. We first establish, in Fig. 1(b), that the magnetic excitations at  $(; ; )$  are indeed gapped below  $T_c$ . Shown are transverse  $Q$ -space scans centered at  $(H; K; L) = (l=2; l=2; 0)$  at an energy transfer of  $\hbar = 1.75$  meV. As expected, there is a clear peak above  $T_c$  at  $T = 26$  K, while the signal is suppressed below  $T_c$  at  $T = 1.8$  K.

In Fig. 2, we see how an applied magnetic field can cause this suppressed signal to reappear. For every scan at a new field, the sample was first heated above  $T_c$  and then cooled in the new field back down to  $T = 1.8$  K; this was done to ensure a macroscopically uniform internal field. At an energy transfer of  $\hbar = 1.75$  meV [Fig. 2(a)], the magnetic excitations are completely suppressed up to  $H = 3$  T, and reemerge at  $H = 3.5$  T. A similar behavior is seen at the slightly higher energy transfer of  $\hbar = 2.0$  meV [Fig. 2(b)]. In this case, the peak is seen to reappear at a lower field of  $H = 1.5$  T.

We summarize these field-dependence results in Fig. 3(a). Here we plot the signal strength (written as the imaginary part of the dynamic susceptibility,  $\chi''$ ) as a function of magnetic field for the two energy transfers, as well as for  $\hbar = 1.5$  meV. The signal strength (corrected for the Bose factor) above  $T_c$  at  $T = 26$  K for  $\hbar = 1.75$  meV is shown as a horizontal dashed line. We see that as the field is increased, the signal strength ap-

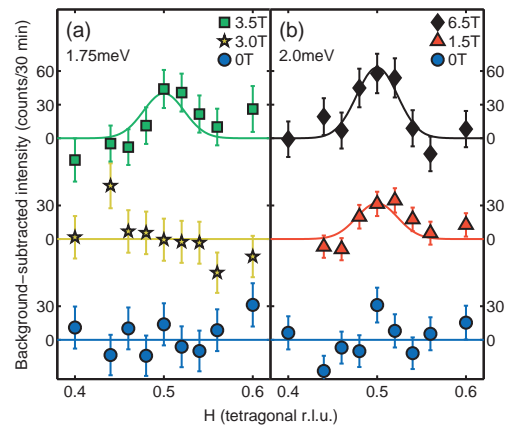


FIG. 2: (color online). (a) Transverse scans  $(H; 1 H; 0)$  about the AF zone center  $(l=2; l=2; 0)$  at an energy transfer of  $\hbar = 1.75$  meV and (b)  $\hbar = 2.0$  meV. Before each scan, the sample was field-cooled from above  $T_c$  to  $T = 1.8$  K. Typical counting time is 30 minutes per point.

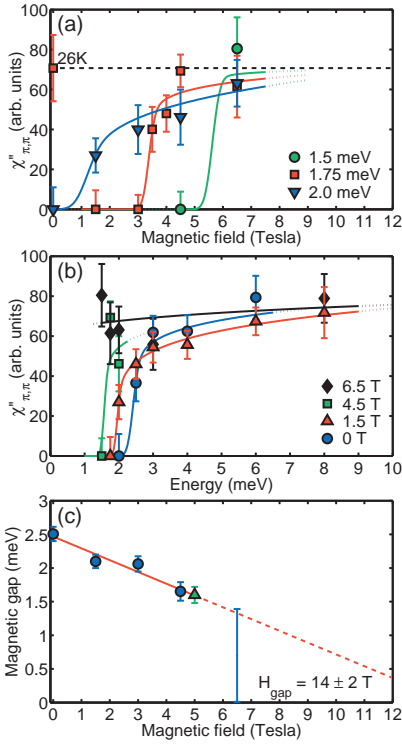


FIG. 3: (color online). (a) Dynamic susceptibility  $\chi''(\omega)$  as a function of eld at several energies. All data are at  $T = 1.8$  K except for the zero-eld datum at  $T = 26$  K. Curves are guides to the eye. (b) The eld-dependence of the magnetic excitation spectrum  $\chi''(\omega)$  versus energy at  $T = 1.8$  K. Curves are guides to the eye. (c) Evolution of the magnetic gap (half maximum energy) as a function of eld. The relation is linear, and extrapolates to a gap-closing critical eld of  $H_{\text{gap}} = 14 \pm 2$  T. The triangle represents data taken at  $H = 5$  T upon zero-eld cooling. Although eld-cooling is preferred (resulting in a uniform internal eld), our result is independent of the cooling method, as might be expected at such high magnetic elds. The vertical bar at  $H = 6.5$  T reflects our limited knowledge that the gap energy is less than 1.5 meV.

proaches this normal-state value.

We plot the magnetic excitation spectrum at several eld values in Fig. 3(b). The zero-eld gap energy in our sample is 2.5 meV, slightly smaller than in previous work [18], in accordance with our somewhat lower  $T_c$ . As the magnetic eld is increased, the gap profile shifts rigidly to lower energies. In particular, note that the signal at lower energies remains zero while the signal is restored by the magnetic eld at slightly higher energies. At our maximum eld of  $H = 6.5$  T, we can no longer discern the gap. Due to a strong increase of the background level at lower energies and the non-zero energy resolution of 1.3 meV (FWHM), we were unable to make measurements below  $\omega = 1.5$  meV. The strong eld-induced background results from the spurious  $(\text{Nd;Ce})_2\text{O}_3$  magnetic elastic signal and from intrinsic paramagnetism of the spin-polarized Nd subsystem of NCCO.

In Fig. 3(c), we plot the gap energy as a function of eld. The magnetic gap decreases linearly with eld, and it completely collapses at an extrapolated value of  $H_{\text{gap}} = 14(2)$  T, consistent with upper critical eld of  $H_{c2} \approx 10(12)$  T [19]. The gapped spectrum of NCCO undergoes a rigid shift towards lower energies as the magnetic eld is increased, which is in stark contrast to the formation of in-gap states in optimally and slightly overdoped LSCO [4, 7]. Because measurements below 1.5 meV have not been possible, it is natural to ask whether the formation of some in-gap states in NCCO could be hidden below this energy. However, we emphasize that the signal strength at 1.5 meV remains zero up until 4.5 T [Fig. 3(a)]. Since our energy resolution is 1.3 meV (FWHM), our experiment is sensitive to any in-gap intensity down to very low energies.

Quite generally, a magnetic eld suppresses superconductivity by orbital pair-breaking of Cooper pairs in the SC state and by lowering the relative energy of the normal state via Pauli paramagnetism of the electron spins [20]. In the orbital pair-breaking limit, the expected zero-temperature critical eld in NCCO is  $H_{\text{orb}} \approx 9$  T, estimated from the slope of  $H_{c2}(T)$  at  $T_c$  [19, 20]. In the Pauli limit, the critical eld is given by  $H_p = \phi_0 / (2e\lambda_B)$ . From measurements of the electronic gap  $\phi_0$  [21, 22], we find  $H_p \approx 30(45)$  T. Since  $H_{\text{gap}} \approx H_{c2} \approx H_{\text{orb}}$ , the response of our sample to a magnetic eld is dominated by orbital effects, namely the balance between the electron kinetic energy and the condensation energy of the Cooper pairs.

We note that our results are not consistent with a singlet-triplet gap, since the Zeeman effect would require a eld of more than 20 T to close the gap. On the other hand, the observed simple linear eld dependence of the magnetic gap is what one obtains in a naive BCS picture of a spatially uniform response. In such a picture, the magnetic gap is proportional to the SC electronic gap, which in turn is proportional to  $T_c$ . According to vortex Nernst effect measurements,  $T_c$  decreases linearly as a function of eld (at least at lower elds) [19]. This implies a linear decrease in the SC electronic gap, as recently measured by Raman spectroscopy [22]. What we have discovered is that the SC magnetic gap also decreases linearly as a function of eld. It is worth noting that our measured magnetic gap of 2.5 meV is much smaller than twice the electronic gap [21, 22]. This suggests a non-trivial relationship between the electronic and magnetic gaps. A possible theoretical explanation for this observation has been put forward recently [23].

While the picture of a uniform response is consistent with our data, we do know that the electronic response is not uniform. The size of the non-SC vortex cores (the SC coherence length) has been estimated to be 58 Å in NCCO [19]. However, we find that the eld-induced low-temperature response remains momentum-resolution limited, which implies that the dynamic magnetic corre-

lations are long-range (at least 200 Å), spanning both vortex-core and SC regions. This provides further evidence that the magnetic low-energy response of NCCO is uniform.

The in-gap signal that is present in LSCO, but absent in NCCO, has been attributed in SO(5) theory to "bound states" in the vortex cores. In this theory, the non-SC vortex cores act as attractive potentials for magnetic excitations [24, 25]. The dynamics of the AF fluctuations can be described by a Schrödinger-like equation, and the in-gap signal seen in overdoped LSCO corresponds to the presence of magnetic bound states in the vortex-core potentials. The absence of an in-gap signal and the linear field dependence of the gap found in our study of NCCO is consistent with the absence of such bound states [25]. Alternatively, the in-gap intensity in LSCO has been attributed to the proximity of the SC to SC + SDW quantum phase transition [10]. In this context, NCCO corresponds to a new region of the phase diagram, far from such a phase transition. Our results indicate that unlike in the hole-doped case, there is no transition to magnetic order before superconductivity disappears.

Our results point to a picture in which the non-SC ground state at fields above  $H_{c2}$  does not possess magnetic order, but is a paramagnet with AF fluctuations. The first piece of evidence is that, in NCCO, applying a magnetic field and increasing temperature have similar effects, and the gap does not appear to close until SC is completely suppressed [13]. Moreover, the signal strength seen at high magnetic fields equals that in the normal state just above  $T_c$ . All of this indicates that the non-SC ground state beyond  $H_{c2}$  resembles the paramagnetic normal state above  $T_c$ .

A second piece of evidence comes from our complementary study of Ni-doped NCCO. Ni-doping is an alternative method of suppressing superconductivity. Upon substituting only about 1% of Cu with Ni, superconductivity in NCCO is completely suppressed [26]. We have performed zero-field measurements of the instantaneous spin correlation length in an oxygen-reduced non-SC sample of 1.5% Ni-doped NCCO. Figure 1(c) shows that this system at low temperatures has a finite correlation length: the momentum-space peaks are considerably broader than the experimental resolution. Clearly, the non-SC ground state in NCCO, induced by Ni-doping, does not have long-range magnetic order.

The absence of magnetic-field-induced in-gap states in  $\text{Nd}_{1.85}\text{Ce}_{0.15}\text{CuO}_4$  and the likely absence of field-induced magnetic order signify an important difference between the electron-doped and hole-doped cuprates; the competing spin (and charge) density wave order (often referred to as "stripes") observed in hole-doped superconductors, especially in materials derived from the high- $T_c$  parent compound  $\text{La}_2\text{CuO}_4$ , prohibits an unobstructed study of

the antiferromagnetically correlated superconductor due to the presence of a nearby quantum critical point. This complication appears to be avoided by the electron-doped materials, which possess the additional experimental advantage of a relatively low upper critical field.

We would like to acknowledge helpful discussions with G. Aeppli, W. J. L. Buyers, R. S. Markiewicz, F. Onufrieva, P. P. Feuty, J. Zaanen, and S.-C. Zhang. The work at Stanford University was supported by DOE under Contracts No. DE-FG 03-99ER45773 and No. DE-AC 03-76SF 00515, and by NSF DMR 9985067. E. M. M. acknowledges support through the NSF Graduate program.

---

greven@stanford.edu

- [1] R. P. Huebener, *Magnetic Flux Structures in Superconductors* (Springer, Berlin, 2001).
- [2] M. A. Kastner, R. J. Birgeneau, G. Shirane, and Y. Endoh, *Rev. Mod. Phys.* **70**, 897 (1998).
- [3] S.-W. Cheong et al., *Phys. Rev. Lett.* **67**, 1791 (1991); K. Yamada et al., *Phys. Rev. B* **57**, 6165 (1998); H. A. Mook et al., *Nature* **395**, 580 (1998).
- [4] B. Lake et al., *Science* **291**, 1759 (2001).
- [5] B. Lake et al., *Nature* **415**, 299 (2002).
- [6] B. K. Haykovich et al., *Phys. Rev. B* **66**, 014528 (2002).
- [7] J. M. Tranquada et al., *Phys. Rev. B* **69**, 174507 (2004).
- [8] K. Yamada et al., *Phys. Rev. Lett.* **75**, 1626 (1995).
- [9] R. G. Ilardi et al., *Europhys. Lett.* **66**, 840 (2004).
- [10] E. Demler, S. Sachdev, and Y. Zhang, *Phys. Rev. Lett.* **87**, 067202 (2001); Y. Zhang, E. Demler, and S. Sachdev, *Phys. Rev. B* **66**, 094501 (2002).
- [11] B. K. Haykovich et al., *Phys. Rev. B* **71**, 220508 (2005).
- [12] P. K. Mang et al., *Phys. Rev. Lett.* **93**, 027002 (2004).
- [13] K. Yamada et al., *Phys. Rev. Lett.* **90**, 137004 (2003).
- [14] H. J. Kang et al., *Nature* **423**, 522 (2003).
- [15] P. K. Mang, S. Larochelle, and M. Greven, *Nature* **426**, 139 (2003).
- [16] P. K. Mang et al., *Phys. Rev. B* **70**, 094507 (2004).
- [17] T. Uefuji et al., *Physica C* **378-381**, 273 (2002).
- [18] D. Petitgrand, K. Yamada, M. Fujita, and T. Uefuji, *Physica C* **408-410**, 778 (2004).
- [19] Y. Wang et al., *Science* **299**, 86 (2003).
- [20] A. Bianchi, et al., *Phys. Rev. Lett.* **89**, 137002 (2002), and references therein.
- [21] H. Matsui et al., *PRL* **95**, 017003 (2005).
- [22] M. M. Qazilbash et al., *Phys. Rev. B* **72**, 214510 (2005).
- [23] F. Onufrieva and P. P. Feuty, *Phys. Rev. Lett.* **92**, 247003 (2004).
- [24] D. P. Arovas, A. J. Berlinsky, C. Kallin, and S.-C. Zhang, *Phys. Rev. Lett.* **79**, 2871 (1997).
- [25] J.-P. Hu and S.-C. Zhang, *J. Phys. Chem. Solids* **63**, 2277 (2002).
- [26] J. M. Tarascon et al., *Phys. Rev. B* **42**, 218 (1990); J. Sugiyama et al., *Phys. Rev. B* **43**, 10489 (1991); B. Jayaram, H. Chen, and J. Callaway, *Phys. Rev. B* **52**, 3742 (1995).